46

The Moisture Source for the Winter Cyclones in the Eastern Mediterranean

P. Alpert and Y. Shay-El

Department of Geophysics and Planetary Sciences

Tel Aviv University, Tel Aviv, 69978, Israel

(submitted March 1991)

ABSTRACT

A superposed Cyprus Low based on 67 ECMWF datasets is employed for the purpose of calculating the diabatic heating and net condensation over the eastern Mediterranean during rain. It is found that the atmospheric engine chooses to absorb the moisture from the Mediterranean in the region east of Crete and then advects it to the convection region over Israel and surroundings. This suggests that artificial rain enhancement in Israel through increase of the Mediterranean heat storage must consider a much further region to the west of the Israeli coast.

1. Introduction

The geographic region where the moisture is supplied to the rain systems in the eastern Mediterranean became recently of increased interest for the regional meteorologists, hydrologists and environmental scientists. One of the reasons for this is the recent acid rain reports in northern Israel, Levin et al. (1990). Another debate strongly related to the moisture source for the rain systems is the suggestion to increase the Mediterranean heat storage by artificially mixing the upper sea layer during summer, Assaf (1985). The latter will supposedly increase rains in Israel.

Although there are some indication based on analyses of isotopic composition of precipitation in the region, Gat and Carmi (1970), Rindsberger et al. (1990), that the Aegean Sea region significantly contributes to the atmospheric moisture, the contributing areas have not yet been quantitatively analyzed. The severe lack of data in the eastern Mediterranean (EM) made it difficult for any estimation of the regions contributing to the moisture in the rain producing systems.

In the recent decade, however, sophisticated 4-D data assimilation systems have been developed, e.g. ECMWF, which rely heavily on unconventional data from satellites (SATEM), aeroplanes (AIREP, AIDS, ASDAR), buoys etc., particularly over data-sparse regions, see e.g. Bengtsson et al. (1988). Consequently, these observations have significantly complemented the data-sets in regions like that of the EM. Further discussion could be found in Alpert et al. (1990a).

In the present study, we have employed the ECMWF initialized datasets for the purpose of a quantitative estimation of diabatic sources in the EM. The period studied was Nov 1982 - Dec 1988 at 00, 12 UTC with horizontal data resolution of 2.5° x 2.5° and seven mandatory levels (1000, 850, 700, 500, 300, 200, 100 HPa). Next section (Sec. 2) describes briefly the set of equations and the method while Section 3 describes the results pertaining to the identification of the major moisture source. In Section 4 we discuss the implication of our results to the plan of rain enhancement by heat storage increase in the EM.

2. Basic Equations

Shay-El and Alpert (1991, hereafter SA) following Yanai et al. (1973) and others have used the thermodynamic energy eq. along with the moisture balance eq. in order to estimate the diabatic forcings in cyclonic circulations over the Mediterranean region. They adopted the residual method for calculating the diabatic heating and the net condensation from the aforementioned equations respectively for winter (Dec-Feb), as well as for a superposition of a relatively large number of

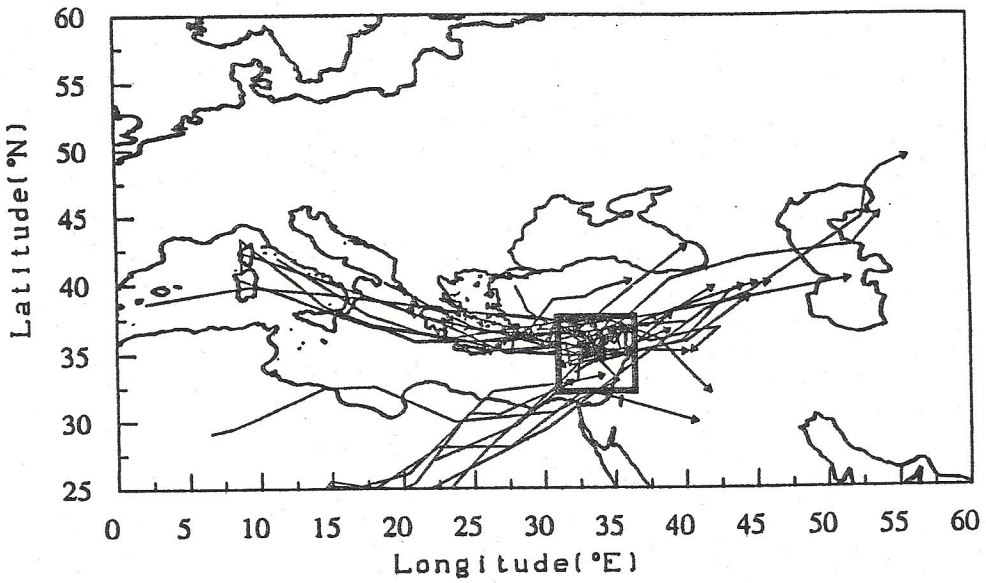

Fig. 1: Cyclone tracks for which the superposed Cyprus low was defined. These tracks were selected out of the 1982-1988 ECMWF dataset based on 4 criterions detailed in the text. The geographic rectangle of 31°-39°E longitude and 32°-38°N latitude referred to in the aforementioned criterions is designated by a heavy line.

EM cyclones. The thermodynamic energy eq. is given in isobaric coordinates per unit mass by:

$$C_P\frac{\partial T}{\partial t} = -C_p\underline{V}\cdot\nabla T - C_P\left(\frac{p}{p_o}\right)^{\kappa}\frac{\partial\theta}{\partial p}\omega + H_T \qquad (1)$$

S_T HA_T VM_T

where:

S_T - storage term,
HA_T - horizontal advection term,
VM_T - vertical motion term,
H_T - diabatic term.

The vertical motion term VM_T is the sum of the vertical advection $(-C_p\omega\frac{\partial T}{\partial p})$ and the adiabatic heating $(RT\omega)/P$. Similarly the moisture balance equation is written as:

$$-L\frac{\partial q}{\partial t} = L\underline{V}\cdot\nabla q + L\omega\frac{\partial q}{\partial p} + H_q \qquad (2)$$

S_q HA_q VM_q

where H_q is the net condensation, i.e. condensation minus evaporation. Common nomenclature is used for the atmospheric variables and constants. The diabatic heating H_T and net condensation H_q, were calculated as residuals in eqs. (1)-(2), see e.g. Yanai et al. (1973), Kasahara et al. (1987).

Following Yanai et al. (1973) or Kuo and Anthes (1984), H_T, H_q can be explicitly written by:

$$H_T = -C_p[\,div\langle T_1\underline{V}_1\rangle - (\frac{p}{p_o})^{\kappa}\frac{\partial\langle T_1\omega_1\rangle}{\partial p}] + Q_R + (3)$$
$$+L(\langle c\rangle - \langle e\rangle)$$

$$H_q = L[\,div\langle q_1\underline{V}_1\rangle - \frac{\partial\langle q_1\omega_1\rangle}{\partial p}] + L(\langle c\rangle - \langle e\rangle) \quad (4)$$

where Q_R is the radiative heating, c and e condensation and evaporation respectively. The $\langle\ \rangle$ parentheses indicate a horizontal average over a grid interval and the subscript 1 stands for subgrid scale perturbations. Hence, the first two terms on the right hand side of (3)-(4) are the contributions due to subgrid scale processes like boundary-layer fluxes, cumulus convection and horizontal diffusion. Since several processes may be responsible for the diabatic heating and the net condensation as shown in eqs. (3)-(4), it may not be completely clear through the residual method what physical process contributes in each case. The present approach, however, which analyzes both H_T and H_q in conjunction with the local circumstances will facilitate the understanding of the prevailing diabatic processes in each instance.

All terms in eqs. (1)-(4) are expressed as heating rates per unit mass and can be translated to daily heating or rate of moisture loss by the following relation

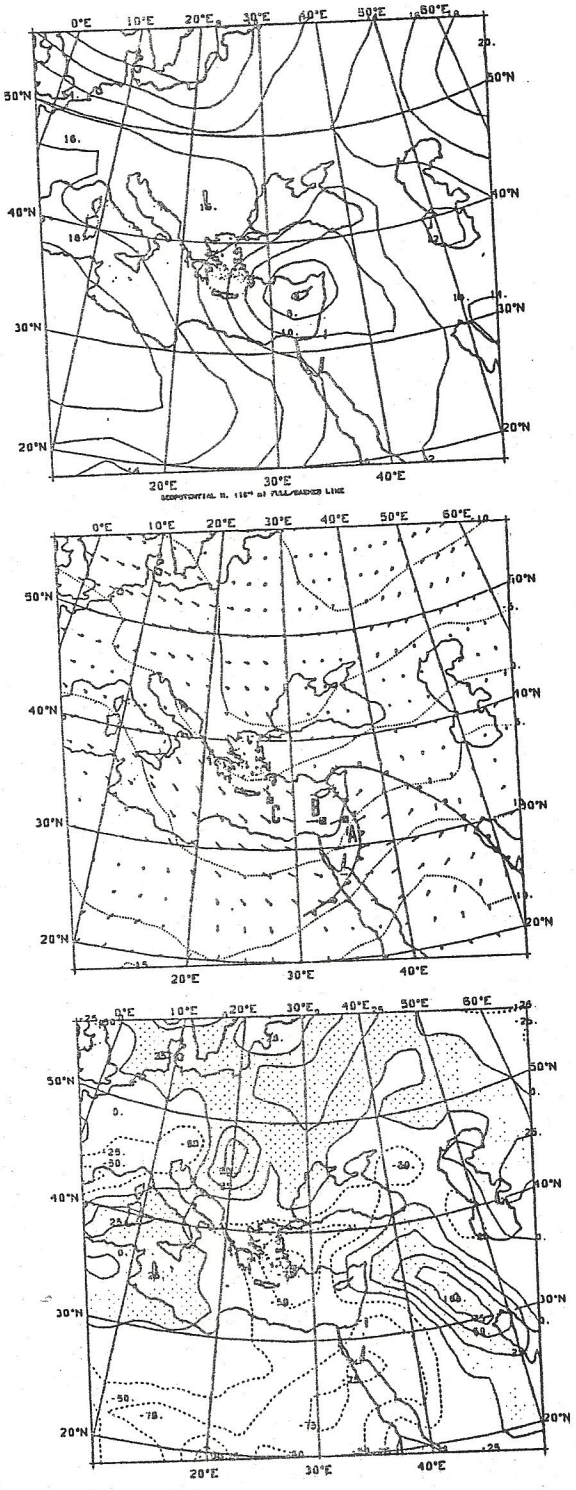

Fig. 2 a-c: Main charts for the superposed Cyprus low as follows: (a) 1000 HPa geopotential height (2dm interval); (b) 850 HPa temperature (dotted, 5K interval) and wind vector arrows representing 6 hr displacements; (c) 850 HPa rate of temperature advection with a $25 \cdot 10^{-3}$ W kg^{-1} interval. Positive (solid) and negative (dashed) contours where positive value regions are shaded. Points A,B,C in Fig. 2b are referenced in text.

$$1 Wkg^{-1} \div 86 Kd^{-1} \div -35\ gr\ kg^{-1} d^{-1} \qquad (5)$$

The vertically integrated heating rates are given per unit area and can be translated similarly for a 900 HPa atmospheric depth (from 1000 to 100 HPa) by,

$$1\ Wm^{-2} \div 10^{-2} Kd^{-1} \div 3.5 \cdot 10^{-3} cm\ d^{-1}. \qquad (6)$$

The right-hand number in (6) is the corresponding rainfall rate when all the heating is directly interpreted in terms of condensation to rainfall water.

The numerical method and the schemes as well as the error estimation are further discussed in SA. The present paper focuses on the significance of the diagnosed moisture sources in the EM.

3. Diabatic Heating/Net Condensation for a Superposed Cyprus Low

a. The Superposed Cyprus Low

Four selective criteria have been applied for the six winters twice a day in order to obtain a meaningful composition of the Cyprus Low. These criterions required a 1000 HPa minimum geopotential height of at least 100 m (equivalent to ~1010 mb in a surface map) found within the EM rectangle drawn in Fig. 1 and during Dec-Feb. In addition it was required that the cyclone was identified in at least 3 consecutive ECMWF datasets. That means having a lifetime longer than 24 hours. Further details about the selection method and track definition are found in Alpert et al. (1990a,b).

Fig. 1 shows the cyclone tracks identified by this method. The region was found cyclogenetic in the sense that cyclones tend to stay longer in the EM. For the current selection 67 sets were found and the average speed of a cyclone along its track was 8.4 ms^{-1} while above the EM rectangle (Fig. 1), it dropped down to an average speed of 4.9 ms^{-1}

Some of the synoptic features of the superposed Cyprus Low are shown in Figs. 2a-c. The 1000 HPa geopotential map, Fig. 2a, shows the cyclone center right over Cyprus. As is well known by local meteorologists the average Cyprus Low is associated with a deep cyclone over the north Atlantic along with a blocking anticyclone over west Europe and northwest Africa. The 850 HPa isotherms (dotted) and wind arrows are presented in Fig. 2b and although 67 sets are averaged, fronts

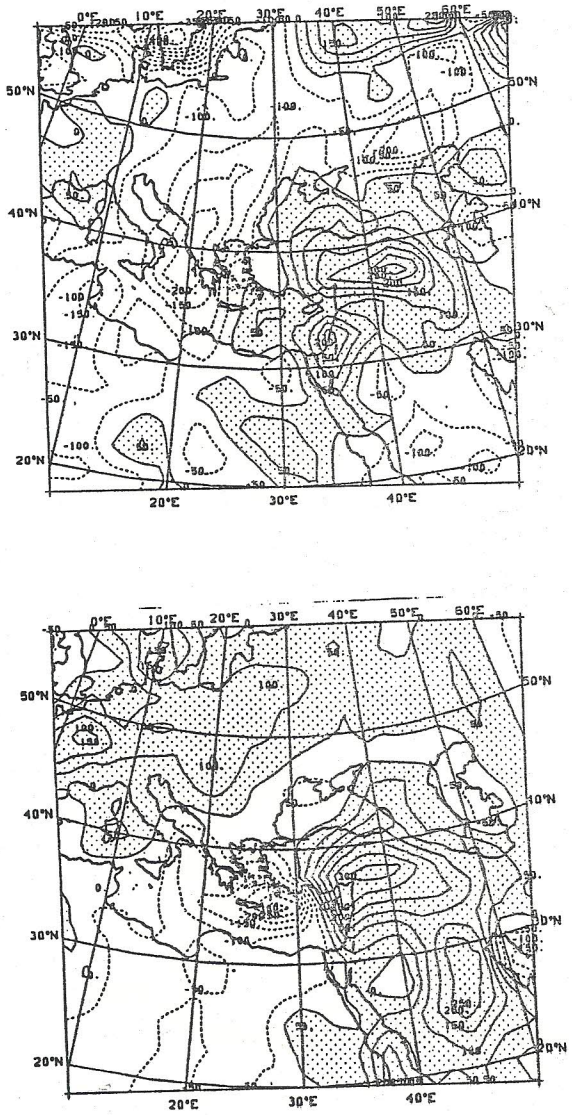

Fig. 3: Distributions of vertically integrated (from the surface to 100 mb) (a) diabatic heating H_T and (b) net condensation H_q for the superposed Cyprus low, based on 1982-1988 ECMWF analyses. Positive (solid) and negative (dashed) contours are plotted in intervals of 50 W m^{-2}. Positive value regions are shaded.

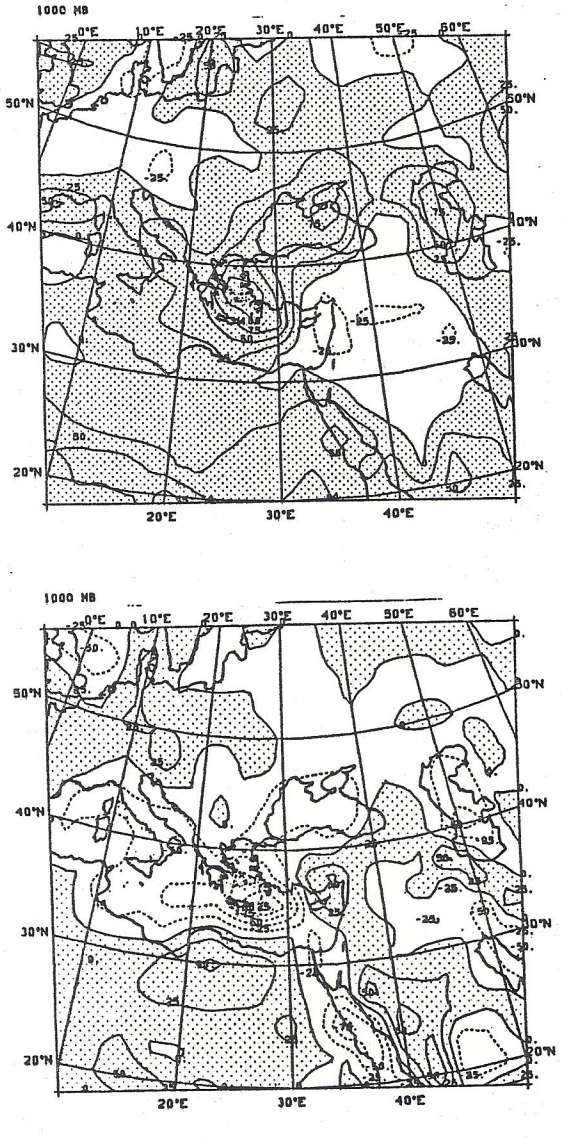

Fig. 4 a-b: As in Fig. 3a-b but for the 1000 HPa surface with a $25 \cdot 10^{-3}$ Wkg^{-1} interval.

can be still clearly identified. The warm and cold fronts were drawn where the 850 HPa maximum warm and cold advection were found respectively, see Fig. 2c.

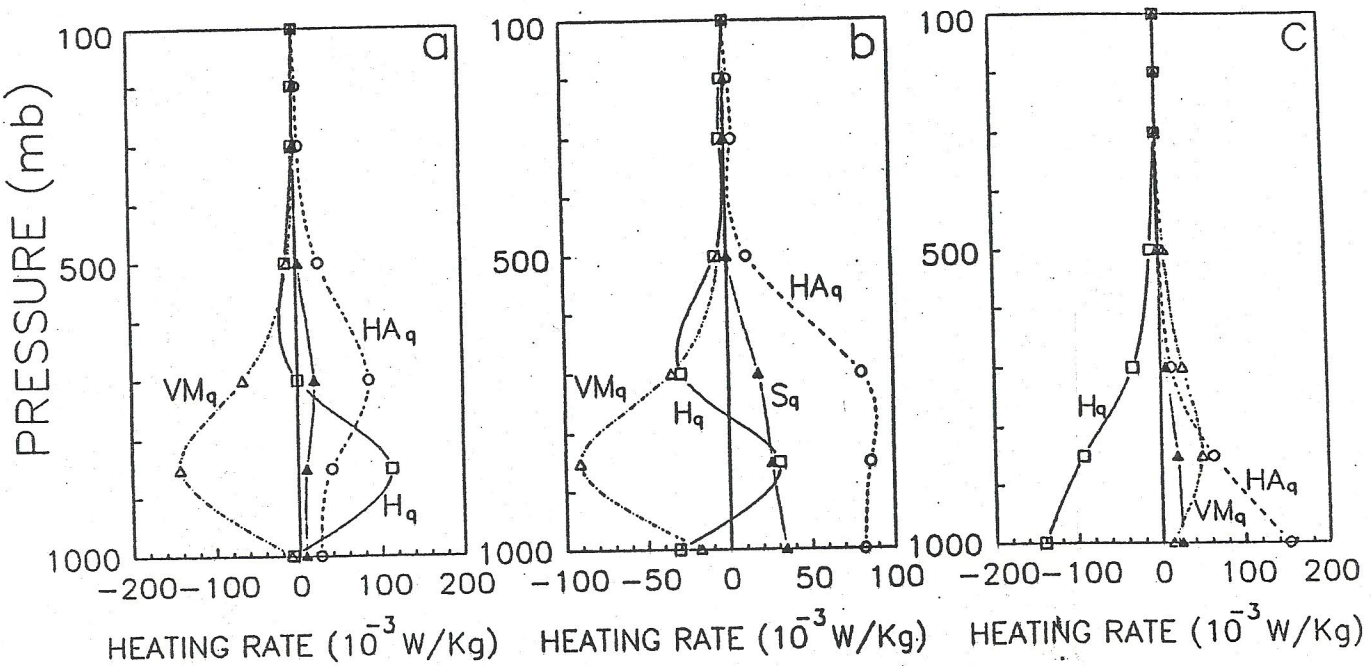

Fig. 5 a-c: Vertical profiles of net condensation H_q (- - -), horizontal advection - HA_q (o--o--o), vertical motion - VM_q (Δ-·-Δ-·-Δ) and storage term - S_q (Δ····Δ····Δ) for the superposed Cyprus low in three selected grid points as follows: (a) 32.5°N, 35°E at the centre of the convective region in the cold front (point A in Fig. 2b); (b) 32.5°N, 32.5°E (point B); and (c) 35°N, 27.5°E at the centre of the downward motion in the wake of the cyclone (point C). Notice the different heating scales.

b. Horizontal distributions of diabatic heating/net condensation

The resulting distributions of the vertically integrated diabatic heating H_T, and the net condensation H_q, for the superposed Cyprus low are shown in Figs. 3a,b. In Fig. 3a two major diabatic heating maxima of 346 and 244 Wm^{-2} appear at the warm and cold fronts respectively. At the high region west of the cyclone the radiative cooling dominates, about 250 Wm^{-2} over west Greece. The net condensation, Fig. 3b, also indicates a major maximum of heating of 329 Wm^{-2} along the warm front. Above the sea the strong turbulent sea surface fluxes result in a net moisture source maximum of -337 Wm^{-2}. This maximum is located right east of Crete and its extension to the Israeli shore probably weakens the cold front maximum associated with the convective latent heat release along the coast, but a maximum line there, could still be noticed. In order to estimate the sea surface turbulent fluxes Figs. 4a-b show the distributions of the diabatic heating/net condensation for the lowest grid level at 1000 HPa. The strongest fluxes are at the lee of the Turkish western mountains probably due to the major contrast between the cold/dry north-northeasterly winds, Figs. 2a,b, and the relatively warm sea. Using the bulk parametrizations for the PBL fluxes over sea,

$$F_T = C_p \rho C_T |\underline{V}|(T_w - T_a) \tag{7}$$

$$F_q = L\rho C_q |\underline{V}|(q_w - q_a) \tag{8}$$

SA calculated the fluxes at the point where the maximum was found, i.e. (35°N, 27.5°E). Substituting the average measured values there, i.e.

mixing ratio at 1000 HPa q_a = 0.0063, sea surface temperature T_w = 17.3°C, air temperature at 1000 HPa T_a = 13.0°C, wind speed $|\underline{V}|$ = 10.6 ms^{-1} and saturated mixing ratio q_w = 0.0123, lead to F_T = 77 Wm^{-2} and F_q = 305 Wm^{-2}. The corresponding integrated values in Figs. 3a-b are H_T = 49 Wm^{-2} and H_q = 337 Wm^{-2}. The reason for H_T being smaller than F_T is mainly explained by the radiative cooling contribution. The good agreement between the sea surface fluxes calculated by the two quite different methods, i.e. the residual method and the bulk parametrization formula lend support to the present method. In SA further comparison is being performed with observed evaporation and precipitation in various points including the tropical region and the NorthBaltic sea and the calculated values seem very reasonable.

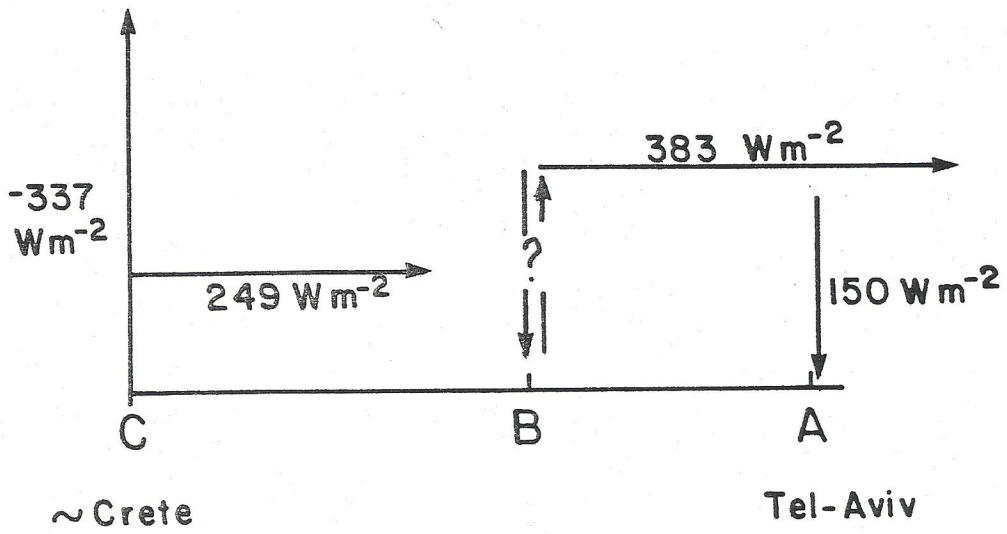

Fig. 6: A schematic presentation by scale of the moisture transport during an averaged Cyprus Low from C through B to A. Vertical arrows show total column net condensation (upward - evaporation only, downward - precipitation only). The horizontal arrows represent the total column net moisture advection downstream.

c. Vertical profiles

In the preceding section (3b) the diabatic heating and the net condensation distributions were compared to show that the major sea surface moisture and heat fluxes during EM cyclones are found to the east of Crete, Figs. 4a-b. They are even strong enough to be reflected in the *integrated* tropospheric column of the diabatic heating and the net condensation (Figs. 3a-b) respectively. In order to directly investigate the vertical distribution of the moisture sources, Figs. 5a-c present the various terms in the moisture balance equation at three EM locations A,B and C, Fig. 2b. It can be seen that these points are positioned along the northwesterly to westerly winds blowing from near Crete (point C), through point B into the Israeli coast, (point A). Although the distances among the points are not large, the differences in the moisture patterns are substantial.

At point A, right on the cold front the moisture vertical transport VM_q is nearly balanced up to about 700 HPa by the net moisture sink H_q, while higher the horizontal advection HA_q removes the moisture. Such a balance between net condensation and the vertical transport of moisture is clearly typical for a major convective region like the tropics, Weare (1988). Unlike the tropical

region the horizontal advection above 700 HPa is significant at the EM coast reflecting the importance of the travelling disturbances. Another difference is the relatively low-level net condensation maximum at ~850 HPa in the convective EM regime. This result suggests the possible importance of including a low-level heating profile when modeling the Mediterranean region in contrast to studies that assume a parabolic heating profile having a maximum higher in the upper half of the cloud, Reed and Recker (1971), Kuo and Anthes (1984).

Moving much further to the west, i.e. east of Crete at point C, where the maximum sea surface fluxes were obtained (Fig. 4b) one can notice a major change of the vertical profiles as shown in Fig. 5c. The H_q profile is negative through the full tropospheric column reaching a maximum at the surface thus indicating a net source of moisture due to the sea surface evaporation. Since the storage term (S_q) at C is small, the net moisture source is mainly balanced by the horizontal advection (HA_q) with an increased contribution of the vertical motion term (VM_q) above 850 HPa. The term VM_q maximizes at ~850 HPa probably the result of the upper level subsidence in that region along with the moisture decrease with height. In summary, point C shows a major moisture supply from the sea surface due to evaporation which is mostly advected to the southeast and partly diluted by the subsidence.

At point B, located about 250 km west to the Israeli coast, Fig. 2b, features seem to exhibit a combination of both characteristics at points C upstream and A downstream. Of particular interest we should point the significant increase of the horizontal advection which also shows an increase at the upper levels of 850 and 700 HPa (compared to C). We interpret this result as the raise of the moisture from the 1000-850 HPa layer at C upwards while moving downstream. Also, the VM_q profile changes sign in comparison with point C indicating initiation of convection (still very weak compared to the convection at the Israeli coast, point A) but the release of latent heat is not yet clearly expressed in the net condensation (H_q).

4. Summary

The basic idea illustrated by the computations here is that the area east of Crete and to lee of the western Turkish mountains, is the major moisture source during the occurrences of Cyprus Low systems in the EM. The moisture supplied to the lower tropospheric levels through evaporation is advected downstream and upwards through the EM (point B). Gradually (at B) some convection develops but the surface evaporation though reduced continues to contribute and the horizontal moisture advection significantly increases to a total of 383 Wm^{-2} at point C. At the Israeli coast (point A) the surface evaporation becomes negligible and the net condensation turns to be significantly positive through the lower troposphere indicating the dominance of convection.

A schematic presentation of the moisture transport during an averaged Cyprus Low in the EM is shown in Fig. 6. These results suggest that if one wants to artificially affect the moisture supply into the rain systems in the EM which are mostly Cyprus Lows, one should relate to the large domain near Crete since this is the area supporting most of the moisture. The large geographic region - Fig. 4b - and its distance from Israel may present serious problems on the logistics and feasibility of such an operation.

5. Acknowldegements

The present work was supported by the GIF (German Israeli Foundation) Grant No. I-138-120.8/89. Thanks to the ECMWF for the data. Thanks to Rachel Duani for typing the manuscript and to A. Dvir for drafting Fig. 6.

REFERENCES

Alpert, P., B.U. Neeman and Y. Shay-El, 1990a: Climatological analysis of Mediterranean cyclones using ECMWF data. *Tellus*, 42A, 65-77.

Alpert, P., B.U. Neeman and Y. Shay-El, 1990b: Intermonthly variability of cyclone tracks in the Mediterranean. *J. Climate*, 3, 1474-1478.

Assaf, G., 1985: Artificial sea mixing. *Israel J. Earth Sci.*, 34, 110-112.

Bengtsson, L., 1988: Advances in the numerical prediction of the atmospheric circulation in the extratropics. *Preprints, Palmen Memorial Sympsium on Extratropical Cyclones*, Amer. Meteor. Soc. Helsinki, 289-291.

Gat, J.R., and I. Carmi, 1970: Evolution of the isotopic composition of atmospheric waters in the Mediterranean Sea area. *J. Geophys. Res.* 75, 3039-3048.

Kasahara, A., A.P. Mizzi, and U.C. Mohanty, 1987: Comparison of global diabatic heating rates from FGGE Level III analyses with satellite radiation imagery data. *Mon. Wea. Rev.*, 115, 2904-2935.

Kuo, Y.-H, and R.A. Anthes, 1984: Semi-prognostic tests of Kuo-type cumulus parametrization schemes in an extratropical convective system. *Mon. Wea. Rev.*, 112, 1498-1509.

Levin, Z., Price, C. and Ganor, E., 1990: The contribution of sulphate and desert aerosol to the acidification of cloud rain in Israel. *Atmospheric Environment*, 24A, 5, 1143-1151.

Reed, R.J., and E.E. Recker, 1971: Structure and properties of synopticscale wave disturbances in the equatorial western Pacific. *J. Atmos. Sci.*, 28, 1117-1133.

Rindberger, M., Sh. Jaffe, Sh. Rahamin and J.R. Gat, 1990: Patterns of the isotopic composition of precipitation in time and space: data from the Israeli storm water collection program, *Tellus*, 42B, 263-271.

Shay-El, Y. and P. Alpert, 1991: A diagnostic study of winter diabatic heating in the Mediterranean in relation with cyclones. *Quart. J.R. Meteor. Soc.*, 117, 715-747.

Weare, B.C. 1988: Diabtic heating in the UCLA general circulation model. *J. Climate*, 1, 704-714.

Yanai, M., S. Esbenson, and J. Chu, 1973: Determination of bulk properties of tropical cloud clusters from large-scale heat and moisture budgets. *J. Atmos. Sci.*, 30, 611-627.